

# Thermal desorption and surface modification of He<sup>+</sup> implanted into tungsten

Zhang Fu <sup>a,\*</sup>, N. Yoshida <sup>b</sup>, H. Iwakiri <sup>b</sup>, Zengyu Xu <sup>a</sup>

<sup>a</sup> Division 111, Southwestern Institute of Physics, P.O. Box 432, Chengdu, Sichuan 610041, China

<sup>b</sup> Research Institute for Applied Mechanics, Kyushu University, Kasuga, Fukuoka 816-8580, Japan

## Abstract

Tungsten divertor plates in fusion reactors will be subject to helium bombardment. Helium retention and thermal desorption is a concerned issue in controlling helium ash. In the present study, fluence dependence of thermal desorption behavior of helium in tungsten was studied at different irradiation temperatures and ion energies. Results showed that helium desorption could start at ~400 K with increasing fluence, while no noticeable peaks were detected at low fluence. Total helium desorption reached a saturation value at high fluence range, which was not sensitive to irradiation temperature or ion energy for the conditions evaluated. Surface modifications caused by either ion irradiation or thermal desorption were observed by SEM. The relationship of surface modifications and helium desorption behavior was discussed. Some special features of elevated irradiation temperature and lower ion energy were also indicated.

© 2004 Elsevier B.V. All rights reserved.

## 1. Introduction

Tungsten is one of the candidate materials for divertor plates of future fusion reactors such as ITER [1,2], due to its good thermal performance. In the case of burning plasma, plasma facing materials will suffer helium ion irradiation and large amount of helium will be implanted into the material. Additionally, helium could be induced into the material by neutron irradiation. The trapped helium will be re-emitted into the divertor chamber by thermal desorption. It is also possible for the released helium to return to the core plasma since the shielding of the transport barrier is not efficient for helium [3]. To estimate the amount of helium re-emission, thermal desorption behavior of helium in tungsten needs to be understood.

Due to insolubility of helium in metals, helium implantation into metal can easily induce helium bubble

formation [4–6]. Helium desorption behavior is largely dependent on bubble growth and burst-out [7–9], which are related to irradiation ion energy, temperature and fluence. In this work, the fluence dependence of thermal desorption behavior of helium in tungsten was studied at different irradiation temperatures and ion energies.

## 2. Experiments

Powder metallurgy tungsten with purity 99.95% was cold rolled to thickness of 0.1 mm. Then specimens were cut to the size of 10 mm × 5 mm. After mechanical and electropolish, specimens were annealed in a vacuum chamber at 2200 °C for 30 min. During annealing, the vacuum was held below 5 × 10<sup>-4</sup> Pa to avoid oxidation.

Helium ion irradiation was conducted with a magnetically separated, mass analyzed ion source. Ion energies were 8, 1 keV and 250 eV. During helium ion irradiation, the specimen temperature was kept at room

\* Corresponding author. Tel.: +86-28 8293 2227; fax: +86-28 293 2202.

E-mail address: [zhangf@swip.ac.cn](mailto:zhangf@swip.ac.cn) (Z. Fu).

temperature or 873 K. The ion fluence was in the range of  $1 \times 10^{20}$ – $3 \times 10^{22}$   $\text{He}^+ \text{m}^{-2}$ . Ion flux was  $1 \times 10^{18}$   $\text{He}^+ \text{m}^{-2} \text{s}^{-1}$  for 8 keV,  $5 \times 10^{17}$   $\text{He}^+ \text{m}^{-2} \text{s}^{-1}$  for 1 keV, and  $3 \times 10^{17}$   $\text{He}^+ \text{m}^{-2} \text{s}^{-1}$  for 250 eV.

After SEM observation to inspect the surface damage caused by helium ion irradiation, helium desorption behavior was studied by Thermal Desorption Spectroscopy (TDS). In the thermal desorption process, specimens were heated by infrared radiation and the temperature was measured by a thermal couple in contact with the specimen surface. The temperature range and ramp rate in TDS were RT  $\sim$ 1600 K and  $1 \text{ K s}^{-1}$ , respectively. The released helium was measured by a QMS (Quadra-pole Mass Spectrometer), which was calibrated with a standard helium leak source before each experiment. When the temperature reached 1600 K, the specimen was freely cooled to RT in the vacuum chamber. Finally, SEM was employed again to identify the surface modification by the thermal desorption process.

### 3. Results and discussions

Thermal desorption spectra for the case of 8 keV irradiation at RT are shown in Fig. 1. Since the ramp rate in thermal desorption was constant at  $1 \text{ K s}^{-1}$  for all specimens, the spectra were converted to desorption rate vs temperature. Total helium desorption, which was calculated from the integral of desorption rate vs time curves, is shown in Fig. 5. Results showed that the desorption behavior suddenly changed at fluence of

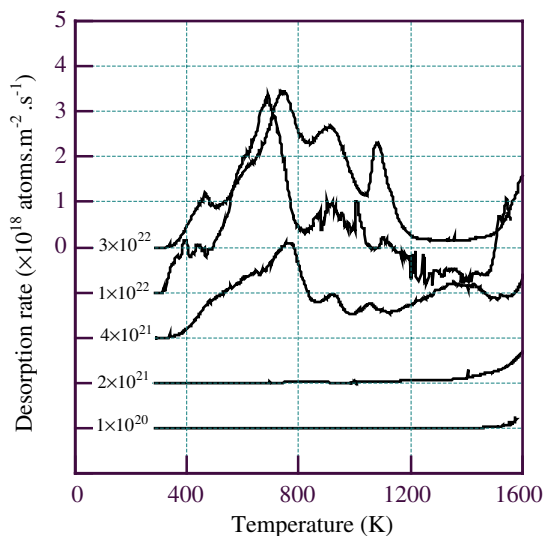


Fig. 1. TDS of specimens irradiated by 8 keV  $\text{He}^+$  at RT with different fluence ( $\text{He}^+ \text{m}^{-2}$ ). The zero line for each TDS line is shifted downward by  $1 \times 10^{18} \text{ He m}^{-2} \text{ s}^{-1}$ .

$4 \times 10^{21} \text{ He}^+ \text{m}^{-2}$ . In the low fluence conditions, helium desorption rates were very low and no obvious peaks were detected. The release peak related to vacancy-He (V-He) clusters [10,11] are known to appear above 1600 K for tungsten. Total helium desorption was much lower than the total implantation and climbed slowly with increasing fluence. When the fluence was  $4 \times 10^{21} \text{ He}^+ \text{m}^{-2}$ , helium desorption started at  $\sim$ 400 K and several peaks appeared below 1600 K. The total helium desorption increased one order of magnitude compared to  $2 \times 10^{21} \text{ He}^+ \text{m}^{-2}$ . With further increasing fluence, the total fraction of helium desorption remained almost the same, although some changes of peak height and position in TDS were noted.

SEM observation indicated that blistering by ion irradiation started at the same fluence of  $4 \times 10^{21} \text{ He}^+ \text{m}^{-2}$ , as shown in Fig. 2(a) and (b). For fluences of  $2 \times 10^{21} \text{ He}^+ \text{m}^{-2}$  or lower, no significant surface modification was identified. Grain boundaries were easily detected due to annealing before ion irradiation. The irradiation blisters were too small to identify further evolution with increasing fluence at RT. Blisters and holes caused by thermal desorption were shown in Fig. 2(c)–(f). In the cases of  $2 \times 10^{21} \text{ He}^+ \text{m}^{-2}$  and below, the density of blisters was low and the size of blisters was large, and no obvious holes were found. When fluence increased to  $4 \times 10^{21} \text{ He}^+ \text{m}^{-2}$ , blisters became much smaller. Small holes appeared at the bottom of the blisters and among them, through which helium was released. With further increasing fluence, the density of blister decreased and the density of holes increased. There were only holes, and no blisters, on some grains in the case of  $3 \times 10^{22} \text{ He}^+ \text{m}^{-2}$ .

These results show that the saturation and desorption behavior change were at the same fluence of irradiation blistering. Similar phenomena were also reported for other metals [7–9,12,13]. It was believed [14,15] that some micro-paths formed along the inter-bubble cracks in the fluence regime that irradiation blisters started to appear. The helium retention could be limited due to the enhanced permeability of helium through the micro-paths. In the thermal desorption, helium could be released by break-through the micro-cracks at lower temperature. The micro-cracks could also make for bubble coalesce at lower temperature and blister fractures at smaller size. The diversity of surface modifications were in agreement with the multiple-peaks in TDS, which revealed different mechanisms of helium release, as discussed by other authors [7–9].

Fig. 3 shows TDS results in the cases of 8 keV irradiation at 873 K. Similar to RT, helium desorption temperature was very high in the case of  $2 \times 10^{21} \text{ He}^+ \text{m}^{-2}$ . In contrast to the multiple-peaks in the RT cases, only one big peak appeared at  $\sim$ 1000 K when the fluence reached  $4 \times 10^{21} \text{ He}^+ \text{m}^{-2}$ , and the desorption rate was about 3 times higher than that in the RT case.

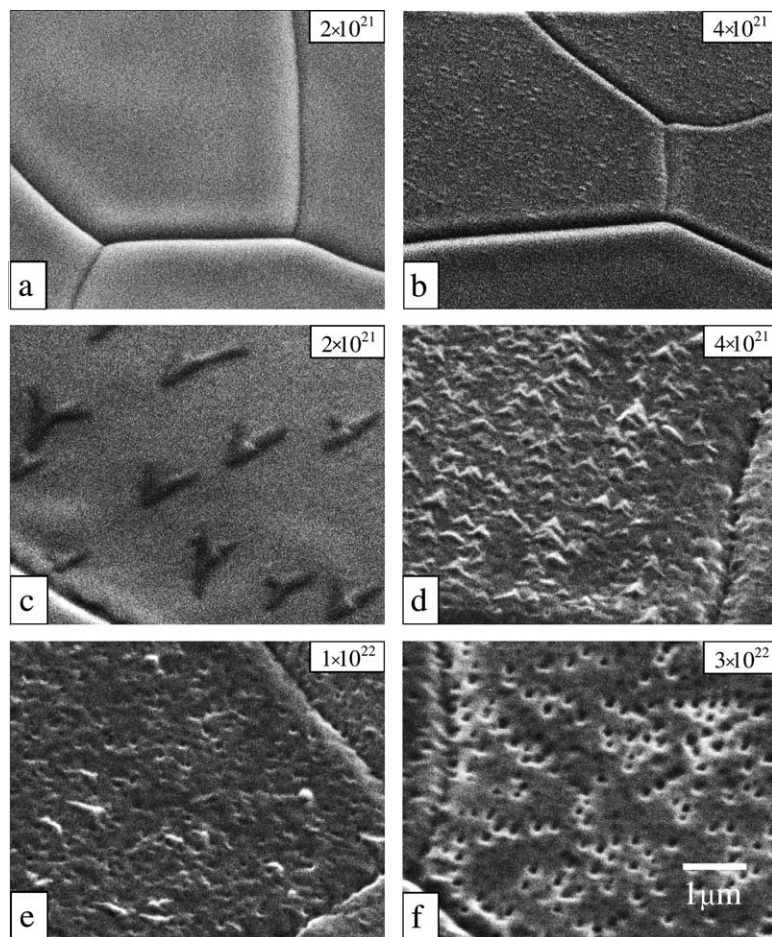


Fig. 2. Surface modifications of specimens irradiated by 8 keV  $\text{He}^+$  at RT to different fluence ( $\text{He}^+ \text{m}^{-2}$ ). (a,b) Before thermal desorption; (c–f) after thermal desorption.

The release peak apparently shifted to lower temperature and grew higher with further increasing fluence. The total desorption was nearly the same as in the RT case.

Surface modifications of the specimens in the cases of 8 keV at 873 K are shown in Fig. 4. Irradiation blistering also started at  $4 \times 10^{21} \text{He}^+ \text{m}^{-2}$ . The blisters were much bigger than that in RT cases, which corresponded to larger bubbles at elevated temperatures [4]. Many blisters flaked to form holes with opened covers. Similar phenomena were also observed on molybdenum [11] by helium ion irradiation. It can be noticed that the blisters grew bigger with further increasing fluence to  $1 \times 10^{22} \text{He}^+ \text{m}^{-2}$ . After thermal desorption, holes developed with very high density and formed a uniform porous structure, which was in agreement with the big peak in TDS. The density of holes also increased with further increasing fluence.

The results showed that total helium retention did not decrease compared to RT cases, although some blisters flaked during irradiation at elevated

temperature. Helium was concentrated in larger bubbles during ion implantation and helium release was mainly controlled by one mechanism in thermal desorption process, which resulted in the large peak in TDS.

The fluence dependent features in the cases of 1 keV at RT were similar to that in the cases of 8 keV at RT. No obvious peaks were detected when fluences were  $3 \times 10^{20} \text{He}^+ \text{m}^{-2}$  or below. Multiple-peaks appeared in TDS starting at  $1 \times 10^{21} \text{He}^+ \text{m}^{-2}$ . No blister was found on any specimens before thermal desorption. The blister size could be too small to be observed by SEM due to the lower ion project range. Blisters and holes were also observed after thermal desorption, but it was difficult to identify the evolution with fluence for the smaller sizes.

As shown in Fig. 5, the saturated helium desorption was  $\sim 1 \times 10^{21} \text{ions m}^{-2}$  for 1 keV cases and  $\sim 1.5 \times 10^{21} \text{ions m}^{-2}$  for 8 keV cases, which was in good agreement with the results by Hino et al. [16]. The change of saturated desorption was very small comparing with that of

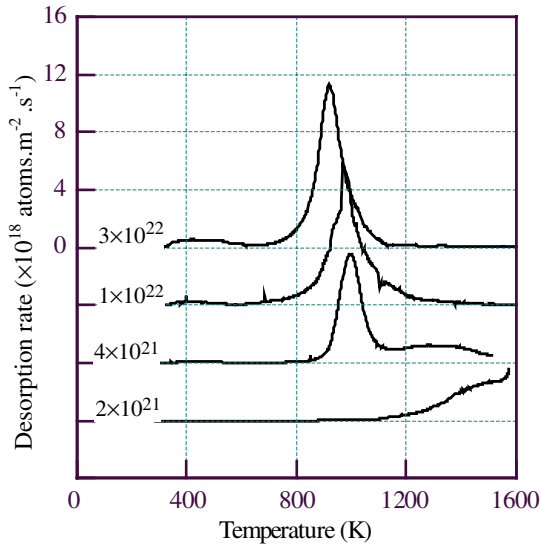


Fig. 3. TDS of specimens irradiated by 8 keV He<sup>+</sup> at 873 K to different fluence (He<sup>+</sup> m<sup>-2</sup>). The zero line for each TDS line is shifted downward by 4 × 10<sup>18</sup> He m<sup>-2</sup> s<sup>-1</sup>.

ion energy. Even in the case of 250 eV irradiation at RT, the total desorption was in the same regime as in higher energy cases. A possible reason was that ion range decreased with decreasing ion energy, however, helium could diffuse deeper into the matrix, because fewer vacancies were produced at the decreased ion energy.

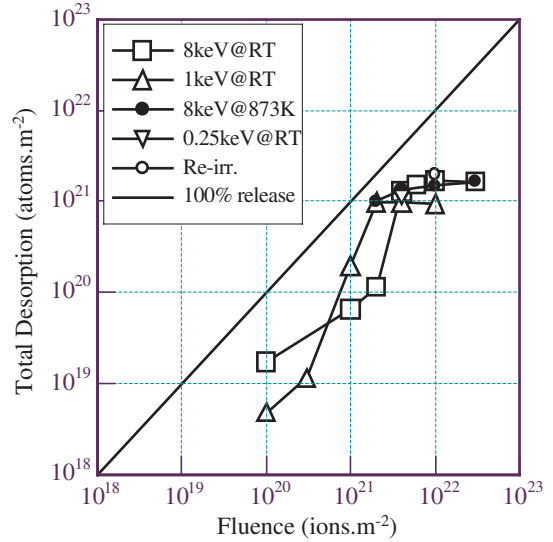


Fig. 5. Total helium desorption in all experimental conditions.

It could also concern the helium retention behavior after thermal desorption, for 1600 K was not sufficient to release all helium in tungsten. After TDS measurement (hence heated to 1600 K, but not re-annealed to 2200 K), the specimen first irradiated by 3 × 10<sup>22</sup> He<sup>+</sup> m<sup>-2</sup> of 8 keV at RT was re-irradiated to 1 × 10<sup>22</sup> He<sup>+</sup> m<sup>-2</sup> by 8 keV at RT. No significant change in total desorption was found, as shown in Fig. 5. The result

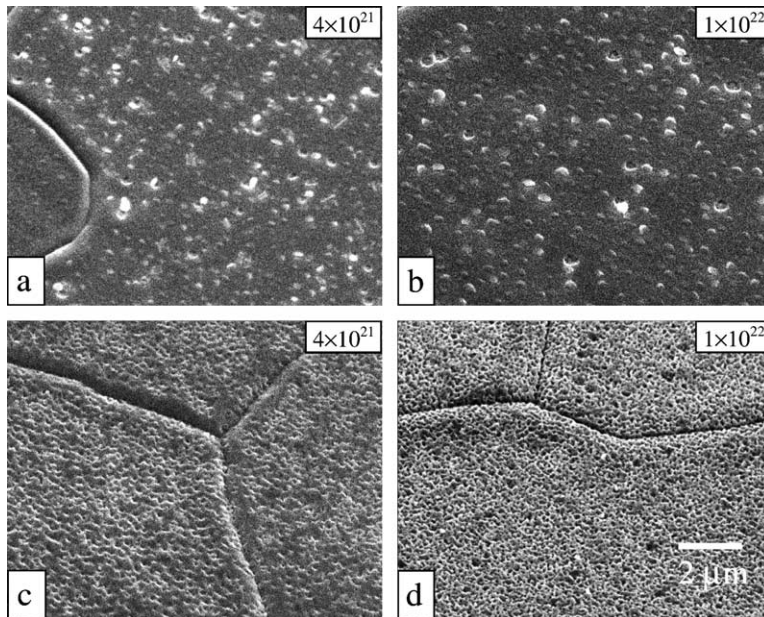


Fig. 4. Surface modifications of specimens irradiated by 8 keV He<sup>+</sup> at 873 K to different fluence (He<sup>+</sup> m<sup>-2</sup>). (a,b) Before thermal desorption; (c,d) after thermal desorption.

could also reflect that the residual helium after thermal desorption was relatively small, as it was indicated by other authors [7–9] that the helium desorption related to V-He clusters was a small fraction in high fluence regime.

#### 4. Conclusions

The fluence dependence of helium desorption was studied at different ion irradiation temperatures and ion energies. Results indicated large amounts of helium could be released in the temperature range of 400–1600 K with increasing fluence. Total helium desorption reached saturation values at the high fluence range, which was not sensitive to irradiation temperature or ion energy in the present conditions. SEM observation showed that blisters could be produced by either ion irradiation or thermal desorption. Thermal desorption behavior was largely related to the blistering during irradiation. Holes and porous structures formed after thermal desorption in high fluence conditions. The large amount of helium desorption, especially the high

desorption rate in the cases of elevated temperatures, could be a disadvantage in controlling helium in fusion reactors.

#### References

- [1] G. Janeschitz et al., *Fusion Eng. Des.* 49&50 (2000) 107.
- [2] R. Aymar et al., *Plasma Phys. Control. Fus.* 44 (2002) 519.
- [3] H.S. Bosch et al., *J. Nucl. Mater.* 290–293 (2001) 836.
- [4] H. Iwakiri et al., *J. Nucl. Mater.* 287–293 (2000) 1134.
- [5] M.I. Baskes et al., *J. Nucl. Mater.* 102 (1981) 235.
- [6] H. Trinkaus et al., *J. Nucl. Mater.* 122&123 (1984) 522.
- [7] V.F. Zelenskij et al., *J. Nucl. Mater.* 151 (1987) 22.
- [8] T. Fukahori et al., *J. Nucl. Mater.* 133&134 (1985) 277.
- [9] T. Yamauchi et al., *J. Nucl. Mater.* 174 (1990) 53.
- [10] G.J. van der Kolk et al., *J. Nucl. Mater.* 127 (1985) 56.
- [11] E.V. Kornelsen, *Radiat. Eff.* 13 (1972) 227.
- [12] T. Yamauchi et al., *J. Nucl. Mater.* 179–181 (1991) 308.
- [13] T. Yamauchi et al., *J. Nucl. Mater.* 189 (1992) 217.
- [14] W.D. Wilson et al., *Phys. Rev. B* 13 (1976) 2470.
- [15] Y. Lifshitz et al., *J. Nucl. Mater.* 137 (1986) 139.
- [16] T. Hino et al., *J. Nucl. Mater.* 266–269 (1999) 538.